

Evolution of $\{001\}\langle 110\rangle$ orientation and related lattice rotation of Al alloy 6111 during rolling

CHEN Yang(陈扬)^{1,2}, TIAN Ni(田妮)¹, ZHAO Gang(赵刚)¹,
LIU Chun-ming(刘春明)¹, ZUO Liang(左良)¹

1. School of Materials and Metallurgy, Northeastern University, Shenyang 110004, China;
2. School of Materials and Chemical Engineering, Liaoning Institute of Technology, Jinzhou 121001, China

Received 28 June 2006; accepted 20 January 2007

Abstract: The texture evolution and lattice rotation in Al alloy 6111 with an initial $\{001\}\langle 110\rangle$ component during symmetrical and asymmetrical rolling were investigated by means of orientation distribution function(ODF). The results show that the as-rolled initial $\{001\}\langle 110\rangle$ orientation evolves into not only the copper orientation but also all the other orientations along the β fiber, including the brass orientation, by lattice rotation around special directions. Compared with the symmetrical rolling, the $\{001\}\langle 110\rangle$ component in the surface layer on the slower roller side evolves more quickly into the orientations along the β fiber during asymmetrical rolling, while that in the surface layer on the faster roller side evolves more slowly.

Key words: Al alloy; symmetrical rolling; asymmetrical rolling; $\{001\}\langle 110\rangle$ orientation

1 Introduction

Usually, the texture of rolled Al alloys consists of the orientations along the β fiber. However, the strong friction between the sheet and the rollers and some special geometrical conditions of deformation create the shear component $\{001\}\langle 110\rangle$ in the surface layer due to the asymmetrical strain[1–4]. Therefore, the texture evolution in materials with an initial $\{001\}\langle 110\rangle$ component during rolling has been a subject of much interest. Great attention has been paid to the deformation behavior and texture evolution of FCC single crystals with an initial $\{001\}\langle 110\rangle$ orientation during rolling and channel die compression by X-ray diffraction, electron back scattering pattern(EBSP) technique and TEM[5–9]. It was found that the $\{001\}\langle 110\rangle$ orientation was unstable and rotated towards the copper orientation $\{112\}\langle 111\rangle$ around the transverse direction(TD) during rolling and channel die compression. At large reductions the $\{001\}\langle 110\rangle$ orientation evolved into two complementary copper components. The Goss component was also observed in copper crystals. However, in the studies on aluminum single crystals only two copper components were observed.

The deformation behavior of the $\{001\}\langle 110\rangle$ oriented grains in polycrystal materials may be different from that of single crystals because of the interaction between grains. LIU and MORRIS[10] investigated the texture evolution of aluminum alloy AA5182 with an initial $\{001\}\langle 110\rangle$ texture during rolling and found that the $\{001\}\langle 110\rangle$ orientation rotated towards the copper orientation with a strong scattering towards S orientation $\{123\}\langle 634\rangle$ at the same time. However, there are few reports on the evolution from the $\{001\}\langle 110\rangle$ orientation to the brass orientation $\{110\}\langle 112\rangle$ during rolling, especially from the $\{001\}\langle 110\rangle$ orientation to other orientations during asymmetrical rolling. The aim of the present work is to examine whether and how the $\{001\}\langle 110\rangle$ orientation in a polycrystal Al alloy evolves into other orientations between S and brass orientation along the β fiber during both symmetrical and asymmetrical rolling. It is very important for comprehending the formation of rolling texture and directing the actual processing of Al alloy sheet.

2 Experimental

The alloy used in the present work was prepared in an electric crucible furnace with 99.9% pure Al,

electrolytic Cu, commercially pure Mg, commercially pure Fe, and other alloys of Al-9.5%Si and Al-9%Mn. The ingot was cast in the copper mould cooled with water, with dimensions of 220 mm×120 mm×30 mm. The chemical composition of the ingot is listed in Table 1.

Table 1 Chemical composition of material tested (mass fraction, %)

Si	Mg	Cu	Mn	Fe
1.15	0.72	0.70	0.27	0.26
Zn	Cr	Ti	Al	
0.16	0.11	0.15	Bal.	

After a two-step homogenization heat treatment at 470 °C for 5 h and 540 °C for 16 h, the ends of the ingot were cut and the surface of the ingot was milled. It was heated to 450 °C and held for 1 h for hot rolling, and then it was hot rolled from 28 mm to 4.6 mm in thickness, with the finishing temperature of about 200 °C. The hot rolled sheets were then cold rolled by symmetrical and asymmetrical rolling, respectively, to various reductions (speed ratio=20/16 for asymmetrical rolling). The draughts (ε_n) and the geometry factors (l, d) of the samples cold rolled are listed in Table 2. Machine oil lubrication was applied during cold rolling.

Table 2 Pass thickness reduction and rolling geometry of samples

Pass	Symmetrical rolling (asymmetrical rolling)		
	Thickness/mm	Draught/%	Geometry factor
0	4.66(4.66)		
1	4.20(4.19)	9.9(10.7)	0.98(0.99)
2	3.73(3.72)	11.2(11.2)	1.09(1.10)
3	3.28(3.27)	12.1(12.1)	1.21(1.21)
4	2.80(2.80)	14.6(14.4)	1.42(1.42)
5	2.34(2.33)	16.2(16.8)	1.62(1.64)
6	1.86(1.86)	20.5(20.2)	1.99(1.97)
7	1.39(1.39)	25.3(25.3)	2.47(2.47)
8	0.93(0.93)	33.1(33.1)	3.27(3.27)

The textures of the surface layers of the cold rolled samples were determined with the X' Pert Pro MRD X-ray diffractometer. Three incomplete (111), (200) and (220) pole figures were measured with Schulz back reflection method, and the orientation distribution functions(ODFs) were calculated from the incomplete pole figures by a two-step method[11] at $l_{\max}=16$. The resulting ODFs were presented in constant φ sections under Roe notation system.

3 Results and discussion

3.1 Evolution from {001}<110> into copper orientation

Fig.1 shows the constant φ sections of ODFs of the hot rolled sheets, showing obvious {001}<110> texture components. Fig.2 shows the $\varphi=45^\circ$ sections of ODFs of the samples symmetrically and asymmetrically cold rolled with various reductions. It can be seen from Fig.2(a) that when the sample is symmetrically cold rolled by 20%, the {001}<110> orientation is slightly strengthened. This is because the thickness d of the sample is large and the length l of the contacting arc between the roller and the sample is short, thus the geometry factor (l, d) is small and the deformation is inhomogeneous (shear strain is created)[12]. In addition, the friction between the roller and the sample also strengthens the {001}<110> orientation[13–14]. For the asymmetrically rolled samples, the {001}<110> orientation is obviously strengthened on the faster roller side, whereas that on the slower roller side is weakened after 20% reduction, as seen in Figs.2(b) and (c). However, with the increase of the deformation, the {001}<110> orientation evolves towards the copper orientation along the θ axis, and finally stops at the copper orientation. This suggests that the {001}<110> orientation evolves gradually into the copper orientation.

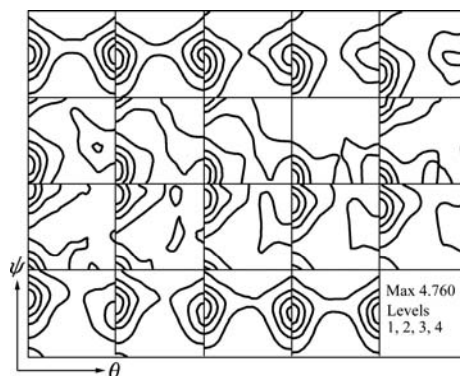


Fig.1 Constant φ sections of ODFs of hot rolled sample

Fig.3 shows the orientation intensities along τ fiber (θ axis of $\varphi=45^\circ$ section) of the samples rolled at various reductions. Figs.3(a) and (b) clearly indicate that the intensity of {001}<110> orientation drops as the reduction exceeds 20% in symmetrically rolled samples and on the faster roller side of the asymmetrically rolled samples, whereas the intensity of the copper orientation is enhanced. In parallel, the intensity peaks shift gradually from the initial {001}<110> towards the copper orientation with increasing of rolling reduction, indicating the evolution from {001}<110> orientation to copper orientation by rotation around the TD.

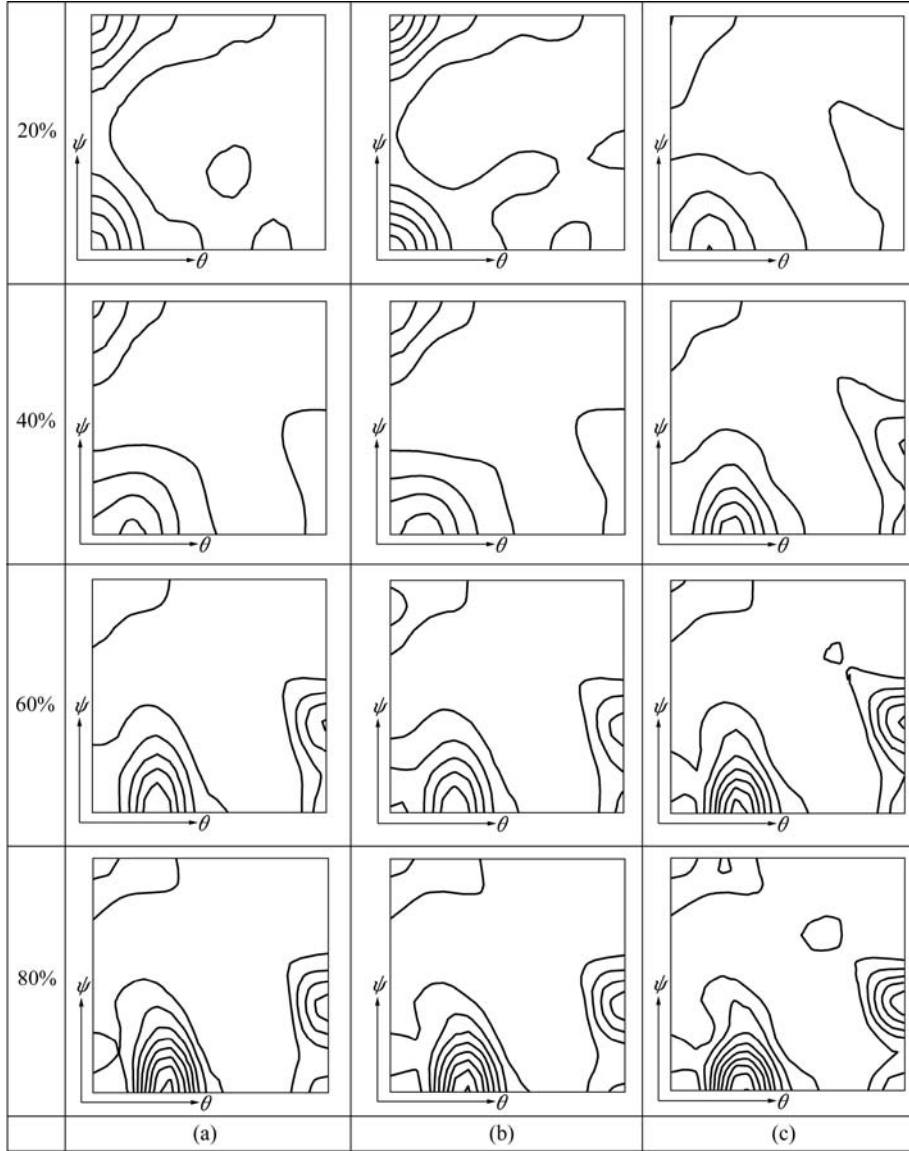


Fig.2 $\varphi=45^\circ$ sections of ODFs of samples symmetrically and asymmetrically cold rolled to various reductions: (a) Symmetrical rolling; (b) Faster roller side of asymmetrical rolling; (c) Slower roller side of asymmetrical rolling

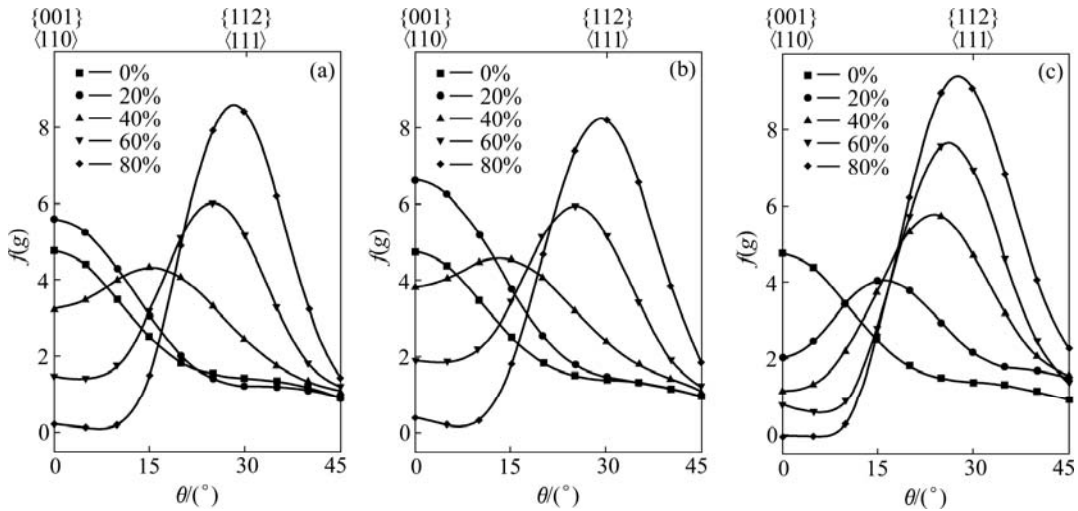


Fig.3 Orientation intensities along τ fiber: (a) Symmetrical rolling; (b) Faster roller side of asymmetrical rolling; (c) Slower roller side of asymmetrical rolling

By comparing Figs.3(c) with Figs.3(a) and (b), it is found that the evolution of $\{001\}\langle 110\rangle$ orientation on the slower roller side is obviously different from that on the faster roller side for the asymmetrical rolling and from that of the symmetrical rolling. When the reduction increases to 20%, the intensities of $\{001\}\langle 110\rangle$ orientations in both symmetrically rolled sample and on the slower roller side of the asymmetrically rolled sample increase, while the intensities of $\{001\}\langle 110\rangle$ orientation on the faster roller side decrease obviously. Moreover, the orientation intensity peaks shift from 0° to 15° , indicating that the evolution from $\{001\}\langle 110\rangle$ to copper orientation on the slower roller side is more quickly than that on the faster roller side and that of the

symmetrical rolling. It shows that in the case of asymmetrical rolling, the shear strain on the slower roller side is very small, and close to plane strain compression, but the shear strain on the faster roller side is very large[15]. Thus, $\{001\}\langle 110\rangle$ orientation on the slower roller side is more unstable and evolves more quickly into other orientations (e.g. copper orientation).

3.2 Evolution from $\{001\}\langle 110\rangle$ orientation to S orientation

Fig.4 shows the $\varphi=25^\circ$ sections of ODFs of the samples rolled at various rolling reductions. It can be seen that as the rolling reduction increases, the $\{001\}\langle 110\rangle$ orientation evolves gradually into S orienta-

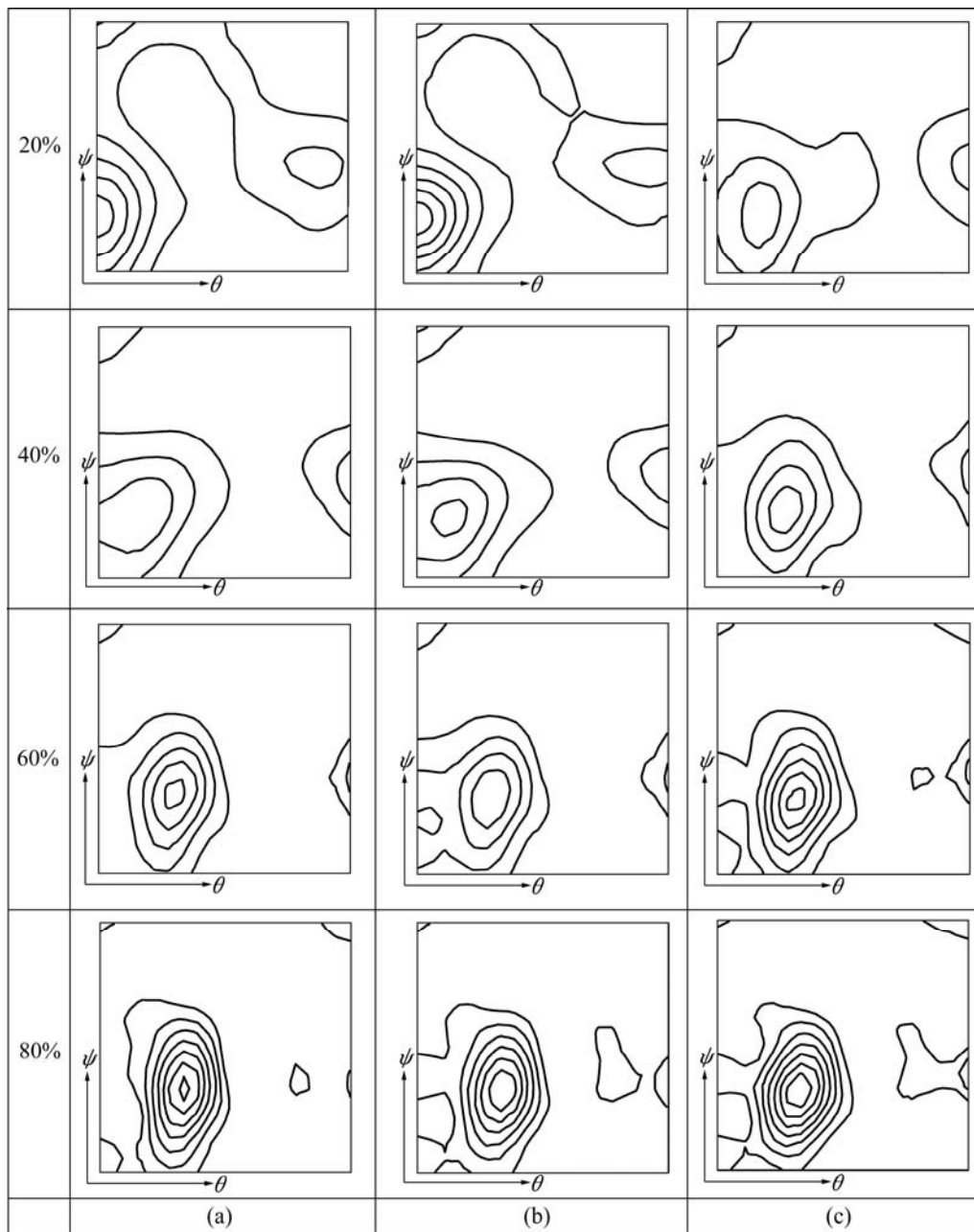


Fig.4 $\varphi=25^\circ$ sections of ODFs of samples symmetrically and asymmetrically cold rolled to various reductions: (a) Symmetrical rolling; (b) Faster roller side of asymmetrical rolling; (c) Slower roller side of asymmetrical rolling

tion. In ODF section at $\varphi=25^\circ$ (Fig.4), the $\{001\}\langle 110\rangle$ orientation is located at $\psi=20^\circ$ and $\theta=0^\circ$, and S orientation is located at $\psi=30^\circ$ and $\theta=30^\circ$. Thus, the lattice rotation during the evolution from $\{001\}\langle 110\rangle$ orientation to S orientation is more complicated than that from $\{001\}\langle 110\rangle$ to copper orientation. For the latter, the lattice rotation is only around TD.

In the case of a cubic system, if the normal direction, rolling direction and traverse direction of an orientation $g=(\psi, \theta, \varphi)$ are respectively D_N, D_R and D_T , it follows

$$D_N = [-\sin\theta \cos\varphi, \sin\theta \sin\varphi, \cos\theta]$$

$$D_R = [\cos\theta \cos\psi \cos\varphi - \sin\psi \sin\varphi, -\cos\theta \cos\psi \sin\varphi - \sin\psi \cos\varphi, \sin\theta \cos\psi]$$

$$D_T = [-\cos\psi \sin\varphi - \sin\psi \cos\varphi \cos\theta, \sin\psi \sin\varphi \cos\theta - \cos\psi \cos\varphi, -\sin\psi \sin\theta]$$

D_N is independent of ψ in the orientation space of $\psi=\theta$ and $\varphi=0-90^\circ$. Therefore the motion of $g=(\psi, \theta, \varphi)$ along a line parallel to ψ axis denotes the rotation of the orientation around ND.

Additionally, for an orientation $g=(\psi, \theta, \varphi)$ in the orientation space, it can prove that the direction that is vertical to ND and intersects TD at ψ of this orientation is

$$\cos\psi D_T + \sin\psi D_R = [\sin\varphi, \cos\varphi, 0]$$

This direction is independent of θ . Thus, the motion of $g=(\psi, \theta, \varphi)$ along the line parallel to axis θ is equivalent to the rotation around a line perpendicular to ND and intersecting TD at ψ .

On the basis of the above analysis, it can be determined that during the evolution from $\{001\}\langle 110\rangle$

to S orientation, the corresponding lattice rotation consists of a 10° rotation around ND and a simultaneous 30° rotation around $[120]$ that is perpendicular to ND and intersects TD at 20° . As the rotation around $[120]$ is accompanied by the rotation around ND, the intersection angle between $[120]$ and TD increases gradually from 20° to 30° , i.e. the rotation axis deviates from the TD and the rotations around ND occur.

The lattice rotation path of the $\{001\}\langle 110\rangle$ to the S orientation evolution can be determined according to the location of orientation intensity peak in the $\varphi=25^\circ$ section of ODFs at different rolling reductions. The intensities of orientations along the orientation rotation path are shown in Fig.5.

It can be seen from Fig.5 that the peaks of orientation intensity along the path from $\{001\}\langle 110\rangle$ to S orientation shift continuously towards S orientation with the increase of the rolling reduction, indicating that numerous $\{001\}\langle 110\rangle$ orientated grains transform into S orientated grains. By comparing Fig.5(c) with Figs.5(a) and (b), it is found that the peak intensities on the slower roller side of the asymmetrically rolled sample shift to S orientation at the rolling reduction of 60% (Fig.5(c)), indicating the completion of the evolution from $\{001\}\langle 110\rangle$ to S orientation, whereas this evolution has not been finished in the symmetrically rolled samples and on the faster roller side of the asymmetrically rolled samples until the rolling reduction of 80% (Figs.5(a) and (b)). This suggests that the evolution from $\{001\}\langle 110\rangle$ to S orientation is quicker on the slower roller side of the asymmetrically rolled samples than that in the symmetrically rolled samples and on the faster roller side of the asymmetrically rolled samples.

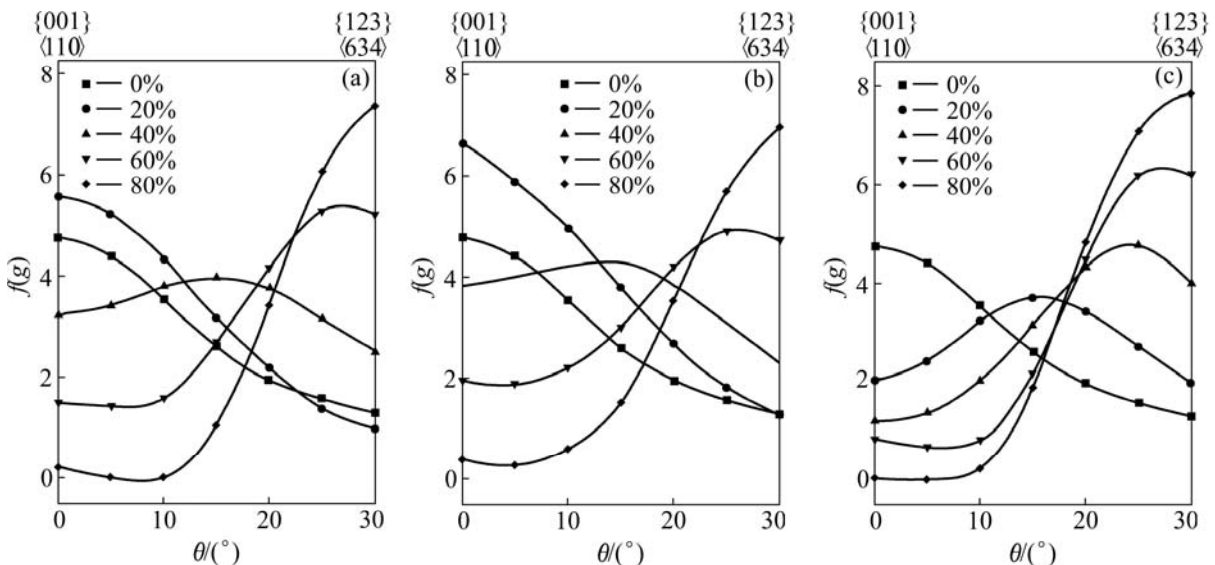


Fig.5 Orientation intensities along orientation rotation path from $\{001\}\langle 110\rangle$ orientation to S orientation: (a) Symmetrical rolling; (b) Faster roller side of asymmetrical rolling; (c) Slower roller side of asymmetrical rolling

3.3 Evolution from $\{001\}\langle 110 \rangle$ to brass orientation

Fig.6 shows the $\varphi=0^\circ$ section of ODFs of the samples rolled at various rolling reductions. It can be seen from Figs.6(a) and (b) that when the rolling reductions exceed 20% for the symmetrically rolled samples and faster roller side of the asymmetrically rolled samples, the $\{001\}\langle 110 \rangle$ orientation spreads gradually towards the brass orientation. The evolution becomes obvious at 40% reduction and the $\{001\}\langle 110 \rangle$ orientation disappears basically at 80% reduction, indicating that a part of the $\{001\}\langle 110 \rangle$ oriented grains

evolve into the brass ones by the lattice rotation; whereas the evolution from the $\{001\}\langle 110 \rangle$ orientation to the brass orientation on the slower roller side of the asymmetrically rolled samples is quick (Fig.6(c)).

The lattice rotation during the evolution from $\{001\}\langle 110 \rangle$ to the brass orientation consists of a 10° rotation around ND and a simultaneous 45° rotation around $[010]$ that is vertical to ND and intersects TD at 45° . The angle between $[010]$ and the TD increases gradually from 45° to 55° , as a result of the rotation around ND. Thus, the deviation from TD of the rotation

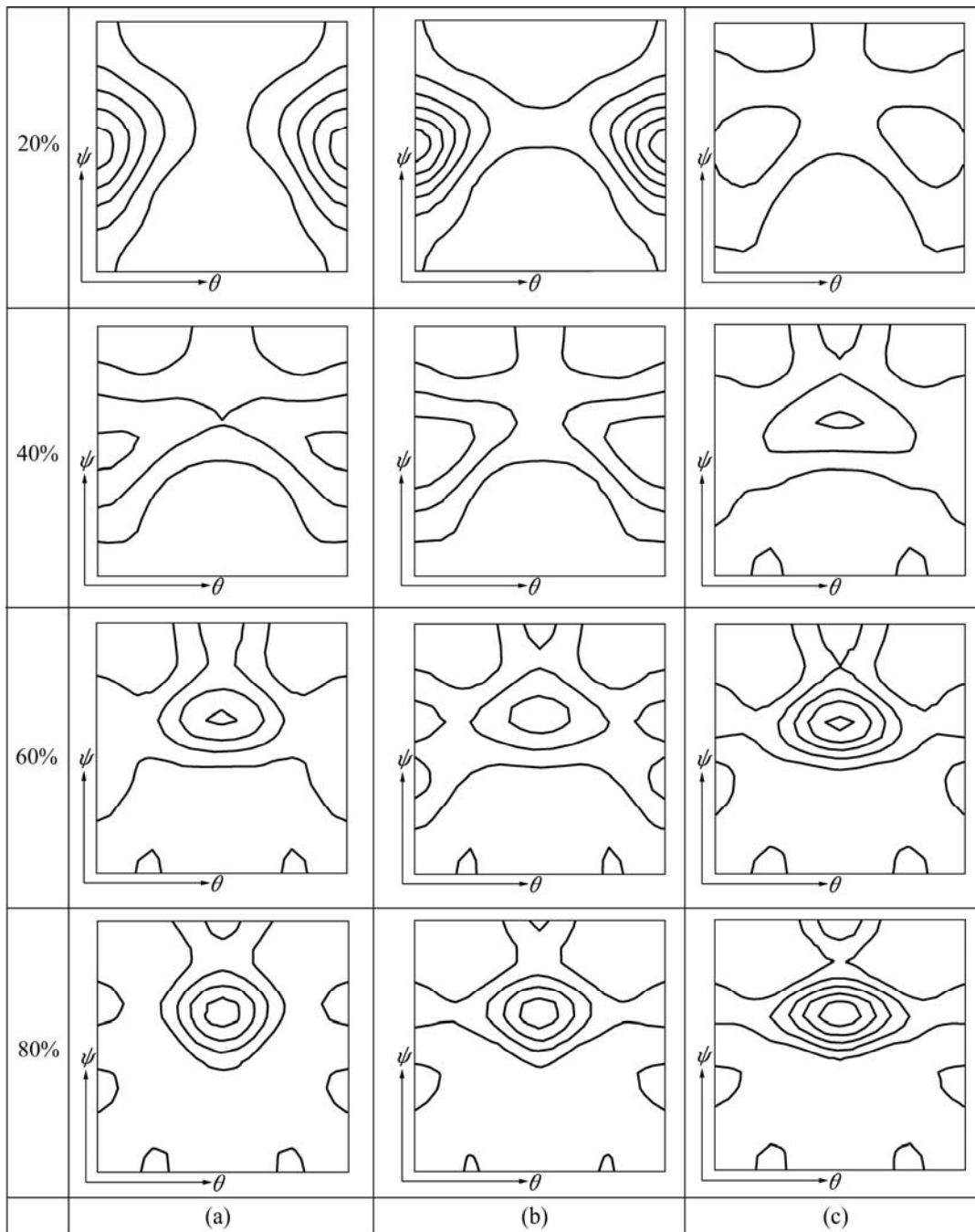


Fig.6 $\varphi=0^\circ$ sections of ODFs of samples symmetrically and asymmetrically cold rolled to various reductions: (a) Symmetrical rolling; (b) Faster roller side of asymmetrical rolling; (c) Slower roller side of asymmetrical rolling

axis during the evolution from the $\{001\}\langle 110 \rangle$ to the brass orientation is more than that during the evolution from $\{001\}\langle 110 \rangle$ to the S orientation. By comparing the evolution from $\{001\}\langle 110 \rangle$ to the brass orientation with that to the copper and the S orientations, it is found that the further the evolved orientation is from the copper orientation, the more the rotation axis deviates from the TD and the more possibly the rotations around ND occur.

Fig.7 shows a zoom ODF section of the symmetrically rolled sample at 40% reduction (Fig.6(a), 40%). The orientation evolution path from $\{001\}\langle 110 \rangle$ orientation to the brass orientation can be determined approximately according to the stretching direction of the intensity-isolines, as shown by the curve with a arrow in Fig.7. The orientation intensities along the orientation evolution path from the $\{001\}\langle 110 \rangle$ orientation to the brass orientation are shown in Fig.8. It can be seen that for symmetrically rolled samples and the slower roller side of the asymmetrically rolled samples, the intensities of the $\{001\}\langle 110 \rangle$ orientation reduce and intensities of the brass orientation increase continuously, when the reductions exceed 20% (Figs.8(a) and (b)), indicating the evolution of some grains from the $\{001\}\langle 110 \rangle$ orientation to the brass orientation. Similar to the evolution from $\{001\}\langle 110 \rangle$ orientation to the copper and S orientations, the evolution from the $\{001\}\langle 110 \rangle$ orientation to the brass orientation on the slower roller side of the asymmetrically rolled samples is quicker (Fig.8(c)). It should be noted that decreasing of the intensity of the $\{001\}\langle 110 \rangle$ orientation does not result uniquely from the evolution into the brass orientation, because of the simultaneous evolution into other orientations such as copper and S. Similarly, and increasing of the intensity of the brass orientation is not

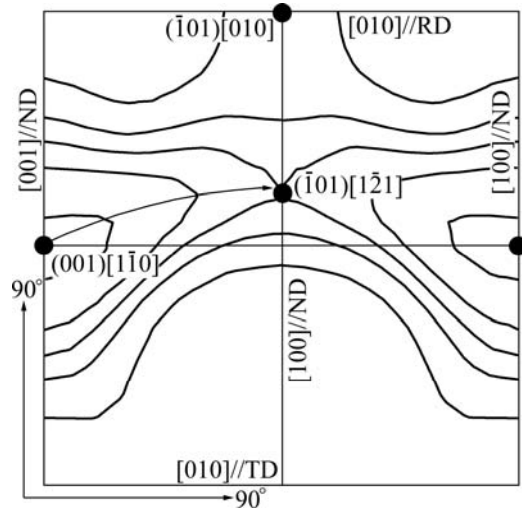


Fig.7 $\varphi=0^\circ$ section of ODFs of sample symmetrically cold rolled to 40% reduction

solely from the evolution of the $\{001\}\langle 110 \rangle$ orientation. It can be seen clearly in Fig.6(a) (60% reduction) that the Goss orientation also evolves into the brass orientation.

Different from Figs.3 and 5, in Figs.8(a) and (b), at 20% reduction, there is no intensified peak shift towards the brass orientation with increasing reduction. This means that the lattice rotation of grains during the evolution from the $\{001\}\langle 110 \rangle$ to brass orientation is not spontaneous, i.e. the $\{001\}\langle 110 \rangle$ oriented grains rotate into the brass orientated ones at different speeds during rolling. The reason is likely that the amount of $\{001\}\langle 110 \rangle$ orientated grains rotating towards the brass orientated ones is less than that rotating towards the copper or S ones, therefore the rotation is easily affected

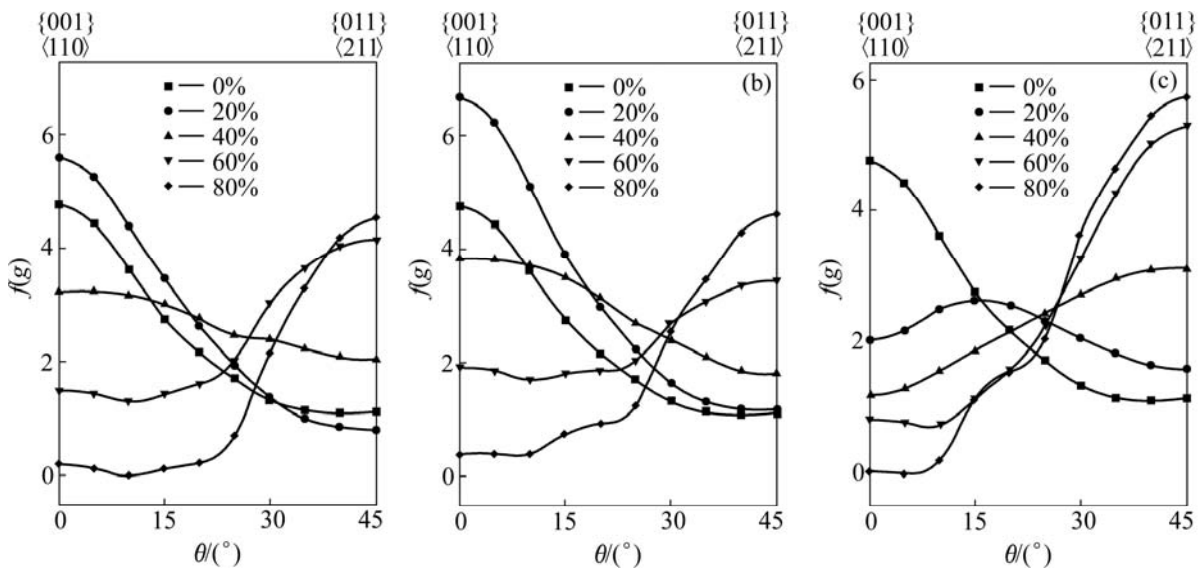


Fig.8 Orientation intensities along lattice rotation path from $\{001\}\langle 110 \rangle$ orientation to B orientation: (a) Symmetrical rolling; (b) Faster roller side of asymmetrical rolling; (c) Slower roller side of asymmetrical rolling

by the neighboring grains.

4 Conclusions

1) The $\{001\}\langle 110 \rangle$ orientation of polycrystal Al alloy is unstable during cold rolling, and evolves gradually into all the orientations along the β fiber including the brass orientation with increase of the rolling reduction.

2) The further the evolved orientation is from the copper orientation, the more the rotation axis deviates from the TD and the more possibly the rotations around ND occur. The lattice is rotated by 30° around TD during the evolution from the $\{001\}\langle 110 \rangle$ orientation to the copper orientation, and it is rotated by 45° around the [010] with a simultaneous rotation of 10° around ND during the evolution from the $\{001\}\langle 110 \rangle$ to the brass orientation.

3) Asymmetrical rolling has strong effect on the evolution of the $\{001\}\langle 110 \rangle$ orientation. The $\{001\}\langle 110 \rangle$ orientation on the slower roller side evolves quicker than that in the symmetrically rolled sample, while that on the faster roller side is slower.

References

- [1] LEE C S, DUGGAN B J. A simple theory for the development of inhomogeneous rolling textures [J]. Metall Trans A, 1991, 22A: 2637–2643.
- [2] ENGLER O, HUH M Y, TOME C N. A study of through-thickness texture gradients in rolled sheets [J]. Metall Mater Trans A, 2000, 31A: 2299–2315.
- [3] PARK J J. Predictions of texture and plastic anisotropy development by mechanical deformation in aluminum sheet [J]. J Mater Proc Technol, 1999, 87: 146–153.
- [4] BHATTACHARYYA A, EL-DANAF E, KALIDINDI S R, DOHERTY R D. Evolution of grain-scale microstructure during large strain simple compression of polycrystalline aluminum with quasi-columnar grain: OIM measurements and numerical simulations [J]. International Journal of Plasticity, 2001, 17: 861–883.
- [5] BAUER R E, MECKING H, LÜCKE K. Textures of copper single crystals after rolling at room temperature [J]. Mater Sci Eng, 1977, 27: 163–180.
- [6] BUTLER JR J F, HU H. Channel die compression of aluminum single crystals [J]. Mater Sci Eng, 1989, A114: L29–L33.
- [7] BECKER R, BUTLER JR J F, HU H, LALLI L A. Analysis of an aluminum single crystal with unstable initial orientation (001)[110] in channel die compression [J]. Metall Trans A, 1991, 22A: 45–58.
- [8] HUMPHREYS F J, ARDAKANI M G. The deformation of particle-containing aluminum single crystals [J]. Acta Metall Mater, 1994, 42: 749–761.
- [9] LI J F, GODFREY A, LIU Q. Microscopic sub-division of rolled Al-1%Mn single crystals of $\{001\}\langle 110 \rangle$ orientation [J]. Scripta Mater, 2001, 45: 847–852.
- [10] LIU W C, MORRIS J G. texture evolution of polycrystalline AA5182 aluminum alloy with an initial $\{001\}\langle 110 \rangle$ texture during rolling [J]. Scripta Mater, 2002, 47: 487–492.
- [11] LIANG Zhi-de, XU Jia-zheng, WANG Fu. Determination of ODF of polycrystalline materials from incomplete pole figures [C]/Proc ICOYOM6. Tokyo, 1981: 1259–1265.
- [12] KNEYSBERG H P, VERBRAAK C A, TEN BOUWHUIJS M J. The influence of inhomogeneous rolling on the capacity of aluminum anode foil material [J]. Mater Sci Eng, 1985, 72: 171–176.
- [13] ZHANG Xin-ming, JIANG Hong-hui, XIAO Ya-qing, CHEN Zhi-yong, LIU Chu-ming, ZHOU Zhuo-ping. Influence of lubricants on deformation textures in high purity Al [J]. The Chinese Journal of Nonferrous Metals, 2001, 11(5): 785–790. (in Chinese)
- [14] DENG Yun-lai, ZHANG Xin-ming, LIU Ying, TANG Jian-guo, ZHOU Zhuo-ping. Effect of deformation geometry and friction on shear texture in high purity aluminum foils [J]. The Chinese Journal of Nonferrous Metals, 2002, 12(4): 634–638. (in Chinese)
- [15] KIM K H, LEE D N. Analysis of deformation textures of asymmetrically rolled aluminium sheets [J]. Acta Mater, 2001, 49: 2583–2595.

(Edited by LI Xiang-qun)